

Synthesis and Reactivity of Molybdenum(IV) Complexes with Alkyl and Aryl Isocyanides

Elon A. Ison, Carlos O. Ortiz, Khalil Abboud, and James M. Boncella*

Department of Chemistry and Center for Catalysis, University of Florida, P.O. Box 117200, Gainesville, Florida 32611-7200, and Chemistry Division, Los Alamos National Laboratory, Los Alamos, New Mexico 87545

Received March 31, 2005

The synthesis and characterization of the bis(isocyanide) complexes $(\text{RNC})_2\text{Mo}(\text{NPh})(o\text{-(Me}_3\text{SiN)}_2\text{C}_6\text{H}_4)$ (**2**: **2a**, R = $t\text{BuNC}$; **2b**, R = 2,6-dimethylphenyl) and the subsequent reactivity of these complexes with excess isocyanide have been reported. An X-ray crystal structure of $(\text{RNC})_2\text{Mo}(\text{NPh})(o\text{-(Me}_3\text{SiN)}_2\text{C}_6\text{H}_4)$ (R = 2,6-dimethylphenyl) is reported. Treatment of **2a** with excess *tert*-butyl isocyanide resulted in the formation of the tris(isocyanide) complex $(t\text{BuNC})_3\text{Mo}(\text{NPh})(o\text{-(Me}_3\text{SiN)}_2\text{C}_6\text{H}_4)$ (**3**). Complex **3** exists in solution in equilibrium with **2a**. Using a two-site exchange mechanism the activation barrier for the dissociative exchange of $t\text{BuNC}$ has been calculated. The X-ray crystal structure of $(t\text{BuNC})_3\text{Mo}(\text{NPh})(o\text{-(Me}_3\text{SiN)}_2\text{C}_6\text{H}_4)$ is reported. Computational studies (ONIOM) performed on **3** reveal that π conflicts in this complex results in the lengthening of the Mo–N(amido)_{cis} bond relative to the Mo–N(amido)_{trans} bond. Treatment of **2b** with excess 2,6-dimethylphenyl isocyanide results in the slow insertion of the isocyanide ligands into the Mo–N bond of the chelating diamide ligand, resulting in a novel chelating iminocarbonyl bis(isocyanide) complex, **4**. An X-ray crystal structure of **4** is reported.

Introduction

In comparison to the well-known insertion of CO and isocyanides, RNC, into metal–alkyl bonds,^{1–3} there are fewer examples of the insertion reaction into metal–amide bonds.^{4–7} The resulting metal–iminocarbonyl derivatives that are formed are important in the general context of amination of organic substrates.⁸ Alkyl isocyanides (RNC) can be regarded as isoelectronic with CO, and their increased ability to act as Lewis bases makes them good candidates to interact with electrophilic metal centers.

Recent work in our group has focused on the use of the chelating disubstituted phenylenediamide group $\{o\text{-(Me}_3\text{SiN)}_2\text{C}_6\text{H}_4\}^{2-}$ ((TMS)₂pda) as an ancillary ligand. The facile high-yield synthesis of several group 6 dialkyl complexes of Mo and W has allowed us to investigate the properties of these metal complexes and determine the influence of this ancillary ligand on their structure,

stability, and reactivity.^{9,10} We have demonstrated that π donation by these ligands is important in stabilizing the metal center and influencing the reactivity of these complexes.^{11–14} Alkyl isocyanide insertion into W–alkyl bonds has been shown to occur readily at room temperature, affording η^2 -imino-acyl complexes that subsequently react via C–C coupling reactions of the η^2 -imino-acyl group, resulting in the formation of diamide ligands.¹⁵

Until now we have not seen any evidence for isocyanide insertion into the metal–amide bonds of the (TMS)₂pda ligand. Isocyanide insertion has been shown to occur preferentially at metal–alkyl bonds as opposed to metal–amide bonds, presumably because of the stronger metal–amide bond.^{5–7,16–19} In this paper, we

* To whom correspondence should be addressed at Los Alamos National Laboratory, P.O. Box 1663, Mail Stop J-582, Los Alamos, NM 87545. E-mail: boncella@lanl.gov. Tel: (505) 665-0795. Fax: (505) 667-9905.

(1) Strauch, H. C.; Wibbeling, B.; Frohlich, R.; Erker, G. *Organometallics* **1999**, *18*, 3802–3812.

(2) Brinkman, K. C.; Blakeney, A. J.; Krone-Schmidt, W.; Gladysz, J. A. *Organometallics* **1984**, *3*(9), 1325.

(3) Durfee, L. D.; Rothwell, I. P. *Chem. Rev.* **1988**, *88*(7), 1059–1079.

(4) Shibata, T.; Yamashita, K.; Katayama, E.; Takagi, A. *Tetrahedron* **2002**, *58*(43), 8661–8667.

(5) Martins, A. M.; Ascenso, J. R.; De Azevedo, C. G.; Dias, A. R.; Duarte, M. T.; Da Silva, J. F.; Veiros, L. F.; Rodrigues, S. S. *Organometallics* **2003**, *22*(21), 4218–4228.

(6) Sanchez-Nieves, J.; Royo, P.; Pellinghelli, M. A.; Tiripicchio, A. *Organometallics* **2000**, *19*(16), 3161–3169.

(7) Wu, Z. Z.; Diminnie, J. B.; Xue, Z. L. *Organometallics* **1999**, *18*(6), 1002–1010.

(8) Holland, P. L.; Andersen, R. A.; Bergman, R. G. *J. Am. Chem. Soc.* **1996**, *118*(5), 1092–1104.

(9) Ortiz, C. G.; Abboud, K. A.; Boncella, J. M. *Organometallics* **1999**, *18*(21), 4253–4260.

(10) Boncella, J. M.; Wang, S. Y. S.; Vanderlende, D. D.; Huff, R. L.; Abboud, K. A.; Vaughn, W. M. *J. Organomet. Chem.* **1997**, *530*(1–2), 59–70.

(11) Mills, R. C.; Abboud, K. A.; Boncella, J. M. *Organometallics* **2000**, *19*(16), 2953–2955.

(12) (a) Cameron, T. M.; Ghiviriga, I.; Abboud, E. A.; Boncella, J. M. *Organometallics* **2001**, *20*(21), 4378–4383. (b) For a comparison of diamide ligand folding in d² and d⁰ complexes see: Ison, E. A.; Cameron, T. M.; Abboud, K. A.; Boncella, J. M. *Organometallics* **2004**, *23*, 4070.

(13) Cameron, T. M.; Abboud, K. A.; Boncella, J. M. *J. Chem. Soc., Chem. Commun.* **2001**(13), 1224–1225.

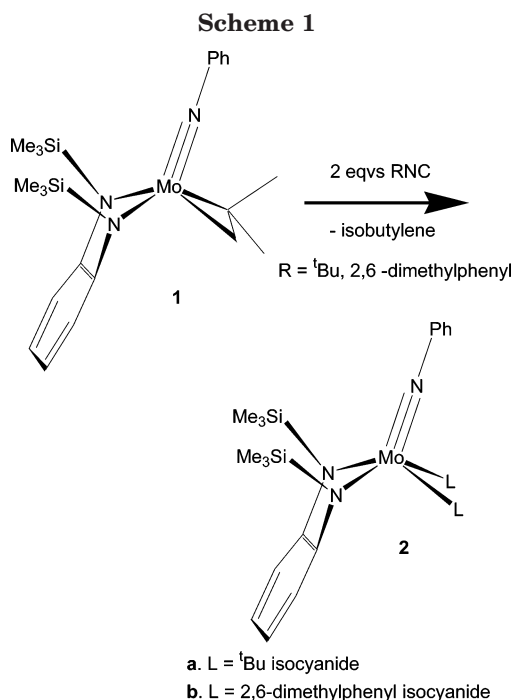
(14) Wang, S. Y. S.; Abboud, K. A.; Boncella, J. M. *J. Am. Chem. Soc.* **1997**, *119*(49), 11990–11991.

(15) Huff, R. L.; Wang, S. Y. S.; Abboud, K. A.; Boncella, J. M. *Organometallics* **1997**, *16*(8), 1779–1785.

(16) Crociani, B. In *Reactions of Coordinated Ligands*; Braterman, P. S., Ed.; Plenum Press: New York, 1986.

(17) Wang, H. P.; Li, H. W.; Xie, Z. W. *Organometallics* **2003**, *22*(22), 4522–4531.

(18) Amor, F.; Sanchez-Nieves, J.; Royo, P.; Jacobsen, H.; Blacque, O.; Berke, H.; Lanfranchi, M.; Pellinghelli, M. A.; Tiripicchio, A. *Eur. J. Inorg. Chem.* **2002**(11), 2810–2817.



report the synthesis and characterization of bis(isocyanide) complexes of Mo and the subsequent reactivity of these complexes with excess isocyanide, yielding tris(isocyanide) complexes in the case of ^tBuNC and an unusual chelating iminocarbamoyl bis(isocyanide) complex in the case of 2,6-dimethylphenyl isocyanide. X-ray structures of a bis(isocyanide) complex, a tris(isocyanide) complex, and the iminocarbamoyl bis(isocyanide) complex are reported.

Results and Discussion

Synthesis of Bis(isocyanide) Complexes. Treatment of a pentane solution of the isobutylene complex (η^2 -isobutylene)Mo(NPh)(*o*-(Me₃SiN)₂C₆H₄) (**1**) with 2 equiv of *tert*-butyl isocyanide resulted in the precipitation of ((^tBuNC))₂Mo(NPh)(*o*-(Me₃SiN)₂C₆H₄) (**2a**) as green microcrystals (Scheme 1). The structure of **2a** has been assigned by ¹H, ¹³C, and IR spectroscopy and is consistent with a square-pyramidal structure, with the imido ligand occupying the apical position as depicted in Scheme 1.

Similarly, treatment of **1** with 2 equiv of 2,6-dimethylphenyl isocyanide afforded ((xylNC))₂Mo(NPh)(*o*-(Me₃SiN)₂C₆H₄) (**2b**; xyl = 2,6-dimethylphenyl), as a dark red crystalline material. Resonances for the SiMe₃ protons are observed at 0.73 ppm (18H), while the RNC (R = 2,6-dimethylphenyl) protons are observed at 2.11 ppm (12H). Two isocyanide stretches in the IR spectrum of **2a** are observed at 2122 (CN symmetric stretch) and 2082 cm⁻¹ (CN asymmetric stretch). The appearance of these stretches at a lower frequency than for the free isocyanide ligand ($\Delta\nu(\text{CN}) = -9$ and -50 cm⁻¹, respectively, where $\Delta\nu(\text{CN}) = (\text{stretching frequency of complex}) - (\text{stretching frequency of free isocyanide})$) is indicative of back-bonding from the metal to the isocyanide ligand.^{16,20} By comparison, the isocyanide stretches for **2b** are observed at 2083 and 2022 cm⁻¹

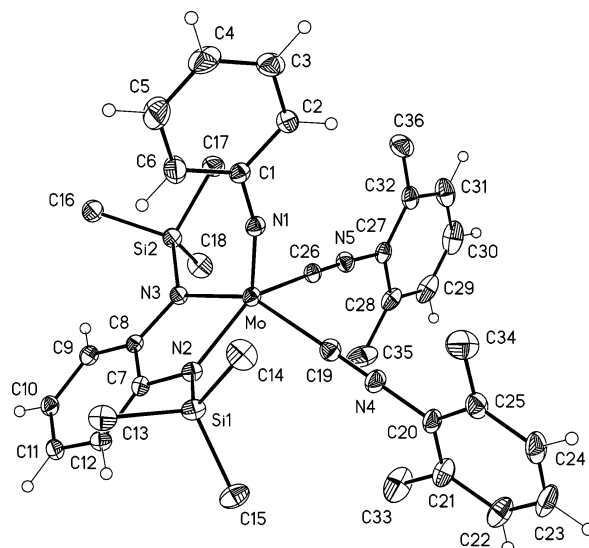


Figure 1. Thermal ellipsoid plot for **2b** (50% probability thermal ellipsoids). Selected bond lengths (Å) and angles (deg): Mo–N(1) = 1.746(2), Mo–N(2) = 2.064(2), Mo–N(3) = 2.093(2), Mo–C(19) = 2.088(3), Mo–C(26) = 2.085(3), C(19)–N(4) = 1.160(3), C(26)–N(5) = 1.166(3); C(19)–N(4)–C(20) = 173.4(3), C(27)–N(5)–C(26) = 176.9(2).

($\Delta\nu(\text{CN}) = -31$ and -92 , respectively). The larger $\Delta\nu(\text{CN})$ values observed for **2b** are reflective of the greater propensity for 2,6-dimethylphenyl isocyanide to act as a π -acceptor ligand. This is in agreement with the observation that aryl isocyanides are better π -acceptor ligands than alkyl isocyanides.¹⁶

X-ray Crystal Structure of 2b. Single crystals of **2b** were obtained by slow diffusion of pentane into a toluene solution of the complex. In addition to the complex, the asymmetric unit contains half of a toluene molecule located on an inversion center. The thermal ellipsoid plot of **2b** is depicted in Figure 1.

The geometry of **2b** is best described as a distorted-square-pyramidal structure with the phenyl imido ligand occupying the axial position. The Mo–N(imido) bond (1.746(2) Å) and the Mo–N(amido) bonds (2.064(2) and 2.093(2) Å) are in the normal range for Mo–N triple bonds and Mo–N single bonds that have been reported in our laboratories.^{10,13,21,22} The Mo–C(isocyanide) bonds (2.088(3) and 2.085(3) Å) are shorter than typical Mo–C(sp) (2.2 Å) bonds in related complexes seen in our group, suggestive of π back-bonding from the metal to the π^* orbital of the isocyanide ligand. The isocyanide ligands are linear, with C–N–C angles of 173 and 177°. As has been reported for other terminal isocyanide complexes, there is no significant increase in the C≡N bond distance (average 1.17 Å).^{23–26}

(20) Ghebreyessus, K. Y.; Nelson, J. H. *Inorg. Chim. Acta* **2003**, *350*, 12–24.

(21) Cameron, T. M.; Ortiz, C. G.; Ghiviriga, I.; Abboud, K. A.; Boncella, J. M. *Organometallics* **2001**, *20*(10), 2032–2039.

(22) Ortiz, C. G.; Abboud, K. A.; Cameron, T. M.; Boncella, J. M. *Chem. Commun.* **2001**(3), 247–248.

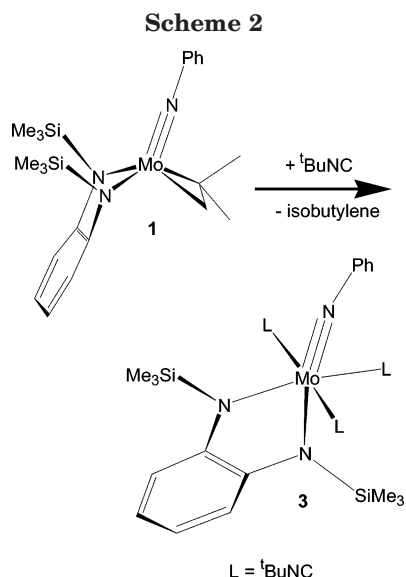
(23) Pombeiro, A. J. L.; Da Silva, C. G.; Michelin, R. A. *Coord. Chem. Rev.* **2001**, *218*, 43–74.

(24) Michelin, R. A.; Pombeiro, A. J. L.; Fatima, M.; Da Silva, C. G. *Coord. Chem. Rev.* **2001**, *218*, 75–112.

(25) Hahn, F. E.; Lugger, T. *J. Organomet. Chem.* **1995**, *501*(1–2), 341–346.

(26) Carofiglio, T.; Floriani, C.; Chiesivilla, A.; Guastini, C. *Inorg. Chem.* **1989**, *28*(24), 4417–4419.

(19) Thirupathi, N.; Yap, G. P. A.; Richeson, D. S. *Organometallics* **2000**, *19*(13), 2573–2579.



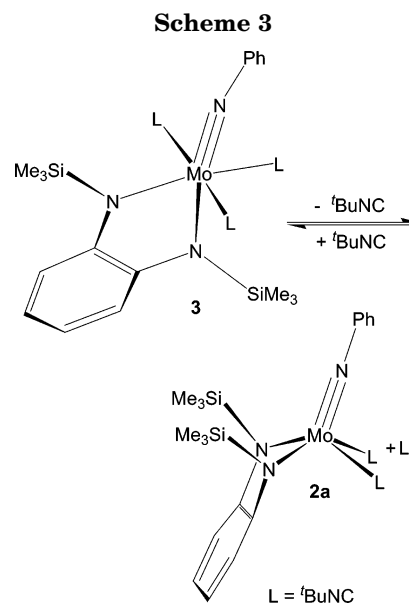
Like the d^2 complexes previously reported in our laboratories, the diamide ligand in this complex is flat (fold angle 173.7°).¹³ The fold angle results from the fact that π donation of the diamide lone pair electrons into the metal d_{xy} orbital is prevented because of the presence of a pair of d electrons in this orbital. The diamide lone pair electrons interact to a lesser extent with the metal d_{yz} and d_{z^2} orbitals because they are destabilized by π donation from the imido lone pair electrons.^{14,27–29}

Synthesis of a Tris (isocyanide) Complex. When **1** was allowed to react with 4 equiv of *tert*-butyl isocyanide, a fast color change from green to purple occurred, and purple microcrystals of the tris(isocyanide) complex (^tBuNC)₃Mo(NPh)(*o*-(Me₃SiN)₂C₆H₄) (**3**) precipitated from solution and were easily isolated by filtration.

The pseudo-octahedral structure of **3**, as shown in Scheme 2, was proposed on the basis of the observed NMR data and confirmed by X-ray crystallography. Resonances corresponding to inequivalent SiMe₃ protons were observed at 0.58 (br s, 9H) and 0.77 ppm (br s, 9H). Broad singlets at 0.93 and 1.17 ppm were assigned to inequivalent *tert*-butyl isocyanide peaks. A plane of symmetry containing the imido nitrogen, (TMS)₂pda nitrogens, and one isocyanide ligand makes the remaining isocyanide ligands chemically equivalent.

The broadening observed in the ¹H NMR spectrum of **3** has been correlated to an equilibrium involving fast, reversible ligand dissociation. As shown in Scheme 3, loss of one RNC ligand induces a plane of symmetry in the bis(isocyanide) complex, **2a**, that is formed. Thus, the remaining isocyanide ligands and the SiMe₃ ligands become equivalent in **2a**. Using the two-site exchange approximation, an activation barrier of $\Delta G^\ddagger = 15.0$ kcal/mol for the ligand dissociation was calculated.

X-ray Crystal Structure of 3. Single crystals of **3** were obtained from slow evaporation of a concentrated pentane solution of **3**. As shown in Figure 2, **3** was found to have a distorted-octahedral geometry. Three iso-



cyanide ligands were found to occupy meridional positions. The imido nitrogen was found to be trans to one of the (TMS)₂pda nitrogens, while the other (TMS)₂pda nitrogen was trans to one of the isocyanide groups. The shorter bond length of Mo–C(24) is attributed to π back-bonding from the metal d orbitals to this isocyanide ligand. Angles around the metal center deviate only slightly from idealized octahedral angles. The smallest angle was the N(2)–Mo–N(3) angle of 77.08° , while the largest angle was N(1)–Mo–N(2) at 106.92° . The acute N(2)–Mo–N(3) angle can be attributed to the small bite angle of the (TMS)₂pda chelate ring.

Complexes **2** and **3** represent rare examples of isocyanide complexes incorporating the isocyanide ligands and the M–N(imido) moiety. While many transition-metal isocyanide complexes have been reported,^{25,26,30} a search of the Cambridge Structural Database revealed only two other examples of complexes incorporating the

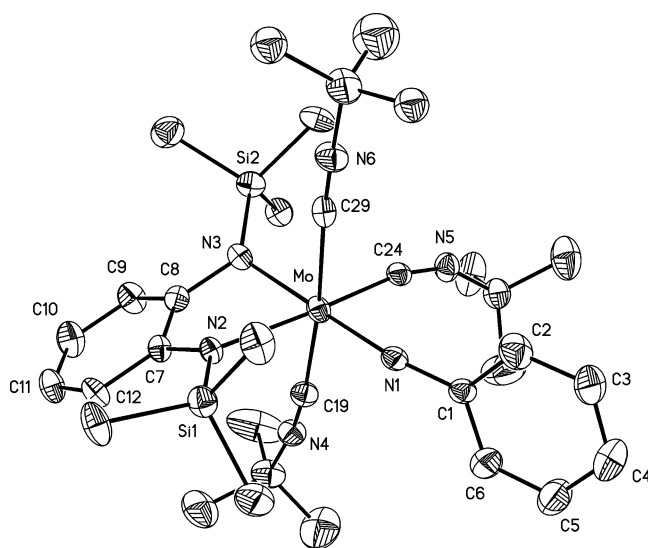


Figure 2. Thermal ellipsoid plot for **3** (30% probability thermal ellipsoids). Selected bond lengths (Å) and angles (deg): Mo–N(1) = 1.804(4), Mo–N(2) = 2.166(5), Mo–N(3) = 2.130(5), Mo–C(24) = 2.067(5), Mo–C(29) = 2.158(5), Mo–C(19) = 2.137(2), –N(2) = 1.182(3); C(2)–N(2)–C(8) = $152.8(5)$.

(27) Del Rio, D.; Galindo, A. *J. Organomet. Chem.* **2002**, 655(1–2), 16–22.

(28) Galindo, A.; Ienco, A.; Mealli, C. *New J. Chem.* **2000**, 24(2), 73–75.

(29) Galindo, A.; Ienco, A.; Mealli, C. *Comments Inorg. Chem.* **2002**, 23(6), 401–416.

imido and isocyanide moieties: the cationic Re complex $[\text{ReCl}(\text{NO}_6\text{H}_4\text{Me-4})(\text{OMe})(\text{tBuNC})_2(\text{PPh}_3)]^{31}$ and the neutral Cr(IV) complex $\text{Cr}(\text{Nmes})(\text{Smes})_2(\text{CNxyl})_2$.³² In addition, the complex $[\text{PhNVCl}_3(\text{tBuNC})_3]$ was reported by Floriani and co-workers.²⁶

The Mo–N(diamide) bonds also reveal an interesting illustration of the π conflicts that arise in complexes incorporating the imido and diamide moieties. The Mo–N(diamide) bonds Mo–N(2) and Mo–N(3) are longer than typical Mo–N(diamide) bonds that have been observed in our group. For example, the Mo–N(diamide) bonds in **3** are significantly longer than the corresponding bonds in both the five-coordinate complex **2b** (vide supra) and the previously reported six-coordinate complex $(\text{THF})\text{Mo}(\text{NPh})(\text{Cl}_2)(o\text{-}(\text{Me}_3\text{SiN})_2\text{C}_6\text{H}_4)$.⁹ In addition, the Mo–N(amido)_{cis} bond, Mo–N(2), is longer than the Mo–N(amido)_{trans} bond, Mo–N(3), at 2.166(5) and 2.130(5) Å, respectively. This trend is also seen in other d² six-coordinate complexes observed in our group. For example, in the previously reported tris(phosphine) complex $(\text{PMe}_3)_3\text{Mo}(\text{NPh})(o\text{-}(\text{Me}_3\text{SiN})_2\text{C}_6\text{H}_4)$,³³ the Mo–N(amido)_{cis} bond is also longer than the Mo–N(amido)_{trans} bond, 2.233(1) and 2.141(1) Å, respectively. These results at first glance appear to be counterintuitive, given the expected trans influence of the imido ligand. However, the elongation of the amido Mo–N_{cis} bond in these complexes results from a filled–filled interaction between an occupied metal d_{xy} orbital and a lone pair on the cis diamide nitrogen.

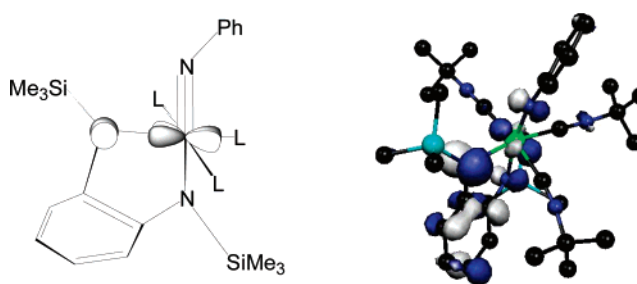
The interaction between the lone pair electrons in the $(\text{TMS})_2\text{pda}$ ligand and Mo was explored by the hybrid DFT method ONIOM, developed by Morokuma and co-workers.^{34–36} For these calculations a two-layer ONIOM method was employed. For the inner layer the *o*-phenylene group (*o*-C₆H₄) that links the two N atoms of the diamido ligand was simplified to a –CH=CH– carbon chain. The organic groups on the nitrogen atoms (SiMe₃ of the amido and phenyl group of the imido) were replaced by hydrogen atoms for simplicity, and the substituents on the isocyanide ligand in **3** were replaced by hydrogen atoms. For this layer the B3LYP/LANL2DZ method was employed. The outer layer consisted of the entire complex, including all substituents on the imido, phenylene diamide, and isocyanide ligands, and was modeled by the B3LYP/LANL2MB method. As shown in Table 1, there is good agreement between the calculated geometries and the crystal structure of **3**.

The presence of an unoccupied orbital on the metal limits the π orbital donation by the diamide ligand. Thus, in the HOMO for **3** (Figure 3) the diamide lone pairs are primarily ligand centered. The energetically unfavorable filled–filled interaction between the diamide ligand and the metal is attenuated somewhat by

Table 1. Selected Bond Lengths (Å) and Angles (deg) for **3**

bond	ONIOM	X-ray
Mo–N(1)	1.824	1.805(3)
Mo–N(2)	2.178	2.166(3)
Mo–N(3)	2.141	2.130(3)
Mo–C(1)	2.149	2.137(5)
Mo–C(2)	2.013	2.067(5)
Mo–C(3)	2.131	2.158(5)
C(4)–N(5)–C(2)	175.5	153.0(4)

the mixing of the metal d_{xy} orbital with the d_{yz} orbital; this brings the d_{xy} orbital slightly out of the xy plane. This repulsive interaction is also minimized in **3**, because of the presence of a π -acceptor ligand trans to the diamide lone pair that can accept electron density from the metal d orbital. In the tris(phosphine), π -acceptor orbitals are not present; consequently the Mo–N(amido)_{cis} bond is significantly longer.



HOMO

Figure 3. Interaction of diamide lone pairs and isocyanide ligand with metal d_{xy} orbitals. (Orbitals are displayed at the 0.05 au isocontour level.)

These results are a further illustration of the consequences of π loading in group 6 imido–diamido complexes that have been emphasized in our group. The competition among π -donor ligands for empty metal π -acceptor orbitals results in the unusual reactivity of these complexes. We believe the weakening of the diamide bonds by the repulsive interaction between the metal and the diamide lone pairs leads to increased reactivity of the diamide ligand (vide infra).

Synthesis, Structure, and Dynamics of a Chelating Iminocarbamoyl Complex. Treatment of a C₇D₈ solution of **2b** with 2 equiv of 2,6-dimethylphenyl isocyanide results in slow conversion (24 h) to the iminocarbamoyl complex **4** (Scheme 4). Complex **4** may be obtained on a preparative scale by treating the metallocyclopentane complex **5**, $(\text{CH}_2)_4\text{Mo}(\text{NPh})(o\text{-}(\text{Me}_3\text{SiN})_2\text{C}_6\text{H}_4)$, with excess 2,6-dimethylphenyl isocyanide (vide supra). The chemical shifts of the SiMe₃ protons occur at 0.44 (s, 9H) and 0.59 ppm (bs, 9H). Signals for the methyl groups of the 2,6-dimethylphenyl isocyanide ligands are observed at 1.94 ppm (s, 12H), and two signals were observed for the 2,6-dimethylphenyl protons at 2.45 (s, 6H) and 1.86 ppm (s, 6H). As shown in Scheme 4, the iminocarbamoyl ligand is coordinated in an η^1 and η^2 fashion to Mo. The chemical shifts for the quaternary carbons of the iminocarbamoyl ligands are observed at 208.2 and 181.4 ppm for the η^2 and η^1 carbons, respectively. One absorption was observed in the IR spectrum for the asymmetric CN stretch (2088

(30) Jameson, G. B.; Ibers, J. A. *Inorg. Chem.* **1979**, *18*(5), 1200–1208.

(31) Ahmet, M. T.; Coutinho, B.; Dilworth, J. R.; Miller, J. R.; Parrott, S. J.; Zheng, Y. F. *Polyhedron* **1996**, *15*(12), 2041–2050.

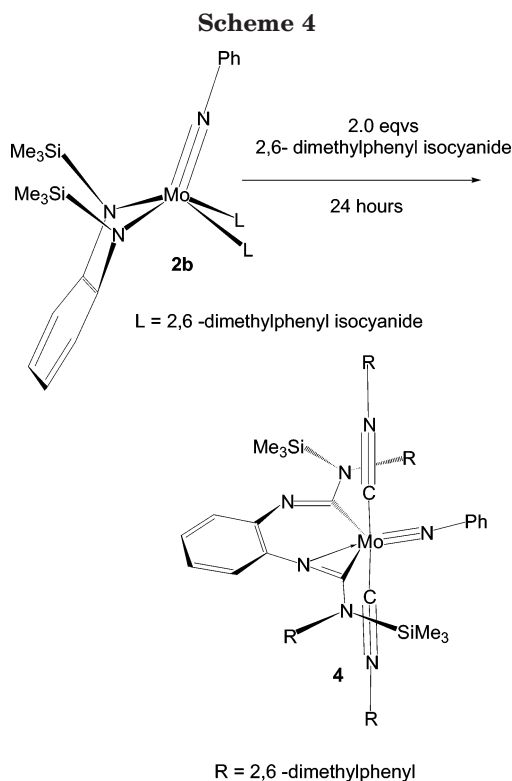
(32) Danopoulos, A. A.; Wilkinson, G.; Sweet, T. K. N.; Hursthouse, M. B. *Polyhedron* **1996**, *15*(5–6), 873–879.

(33) Cameron, T. M.; Ortiz, C. G.; Ghiviriga, I.; Abboud, K. A.; Boncella, J. M. *J. Am. Chem. Soc.* **2002**, *124*(6), 922–923.

(34) Vreven, T.; Morokuma, K. *J. Comput. Chem.* **2000**, *21*(16), 1419–1432.

(35) Vreven, T.; Morokuma, K. *J. Chem. Phys.* **2000**, *113*(8), 2969–2975.

(36) Vreven, T.; Morokuma, K. *J. Chem. Phys.* **1999**, *111*(19), 8799–8803.



cm^{-1}) at a lower frequency than for the free isocyanide ($\Delta\nu(\text{CN}) = -25 \text{ cm}^{-1}$), again suggestive of net π back-bonding in these complexes.

Isocyanide insertion into metal–amide bonds has been less extensively studied than the related insertion reactions into metal–alkyl bonds. In recent years, studies of isocyanide insertions into Ta–amide bonds have been reported.^{6,18,37,38} We propose that the formation of **4** from **2b** occurs by initial coordination of two isocyanide ligands, followed by the rapid insertion of the isocyanides into the metal–amide bond. A 1,3-silatropic shift then follows, and the resulting iminocarbamoyl

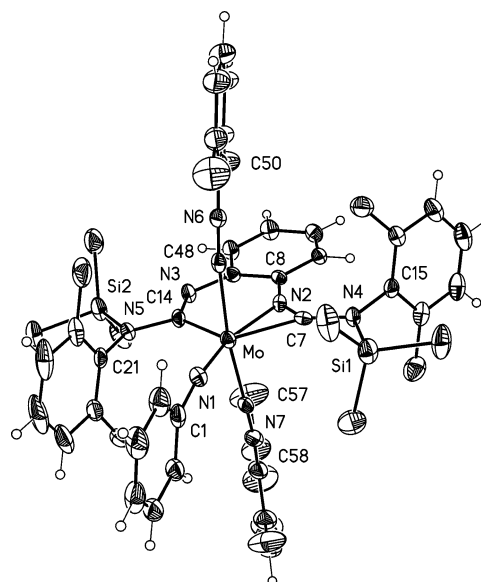
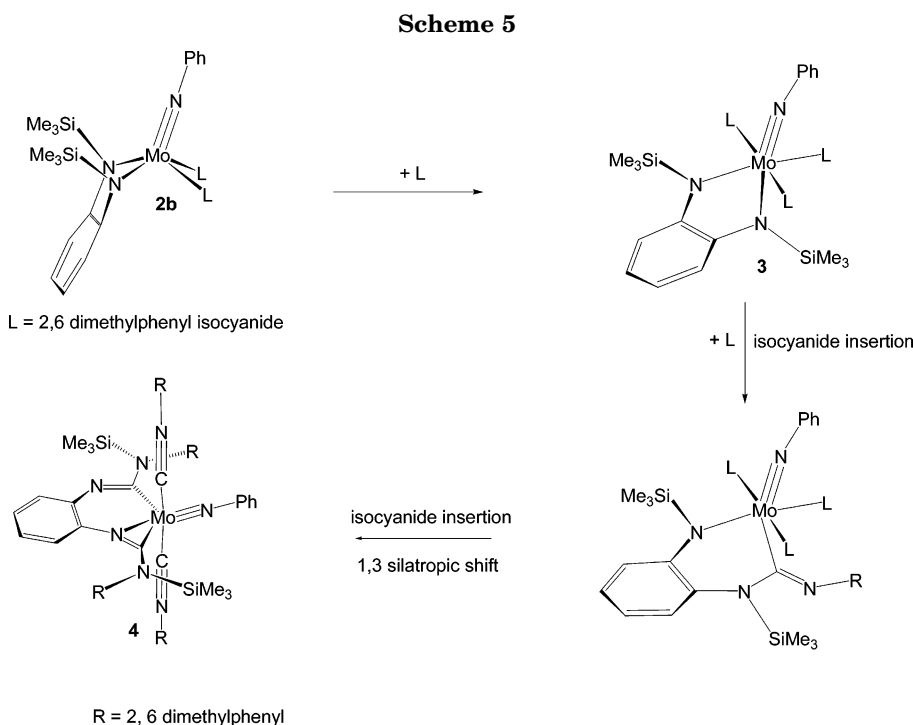
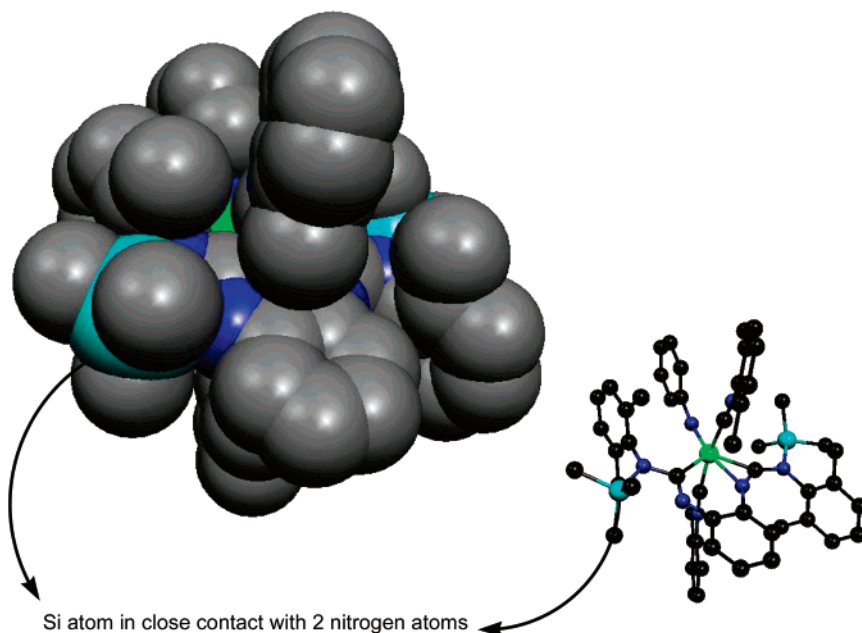


Figure 4. Thermal ellipsoid plot for **4** (30% probability thermal ellipsoids). Selected bond lengths (Å) and angles (deg): Mo–N(1) = 1.767(2), Mo–N(2) = 2.108(2), Mo–C(57) = 2.110(3), Mo–C(48) = 2.131(3), Mo–C(14) = 2.147(3), Mo–C(7) = 2.052(3), N(2)–C(7) = 1.274(3), N(3)–C(14) = 1.318(4), N(4)–C(7) = 1.365(3), N(4)–C(15) = 1.454(3); C(21)–N(5)–C(14) = 124.4(3), C(14)–N(5)–Si(2) = 113.4(2), Si(2)–N(5)–C(21) = 122.1, C(57)–N(7)–C(58) = 166.9, C(48)–N(6)–C(49) = 171.8(3).

species is rapidly trapped by two molecules of 2,6-dimethylphenyl isocyanide (Scheme 5).

X-ray Crystal Structure of 4. Single crystals of **4** were obtained by cooling a concentrated pentane solution of **4** to 0 °C (Figure 4). The geometry about Mo may best be described as a distorted trigonal bipyramid, with the isocyanide ligands occupying the axial position and the iminocarbamoyl fragments and the imido ligand occupying the equatorial plane. A plane of symmetry bisects the two trans isocyanide ligands and passes





Si atom in close contact with 2 nitrogen atoms

Figure 5. Space-filling diagram generated from the crystal structure of **4**. The Si–N bond distances (1.78 and 2.53 Å) are within the sum of the van der Waals radii of N and Si atoms (3.60 Å).

through the imido and iminocarbamoyl fragments. The iminocarbamoyl fragment is flat (rms = 0.02); consequently, the substituents on the amido nitrogens (N(5) and N(4)) are sterically encumbered (vide infra).

The Mo–N(1) bond length (1.767(2) Å) is within the normal range for a molybdenum–nitrogen triple bond. One iminocarbamoyl fragment binds in an η^1 fashion to the Mo center and shows localized C–N bonds: i.e., one short C=N bond, (C(14)–N(3), 1.318(4) Å) and one long C–N single bond (C(14)–N(5), 1.454(3) Å). The η^2 -iminocarbamoyl fragment exhibits a very short C–N bond (C(7)–N(2), 1.274(3) Å) and a long C–N bond (C(7)–N(4), 1.365(3) Å). Both of the amido nitrogens N(4) and N(5) are sp^2 hybridized, with carbon–nitrogen bond lengths shorter than those typically seen for C–N single bonds (1.48 Å), and the sum of the angles around each nitrogen is equal to 359.9°. This suggests delocalization within the CNC framework of the iminocarbamoyl group. The bond lengths for the isocyanide ligands (average 2.12 Å) are shorter than typical Mo–C(sp^2) bonds, suggestive of π back-bonding to isocyanide in these complexes. The C–N–C isocyanide bond angles deviate only slightly from linearity (average 169.4°).

The space-filling model of **4**, generated from the X-ray study, reveals a very sterically congested region in the plane of the iminocarbamoyl fragment (Figure 5). This suggests that free rotation about the carbon–nitrogen bonds C(7)–N(4) and C(14)–N(5) is restricted because of steric hindrance around the nitrogen atoms. For this same reason free rotation of the xyllyl fragments about N(4) and N(5) is restricted because of steric interactions. The silicon atom Si(2) is located close to two nitrogens; this atom is directly bonded to N(5) (bond length 1.78 Å) but is also close to N(3) (2.53 Å). The latter distance is less than the sum of the van der Waals radii of a nitrogen and a silicon atom (3.60 Å), and as is evident

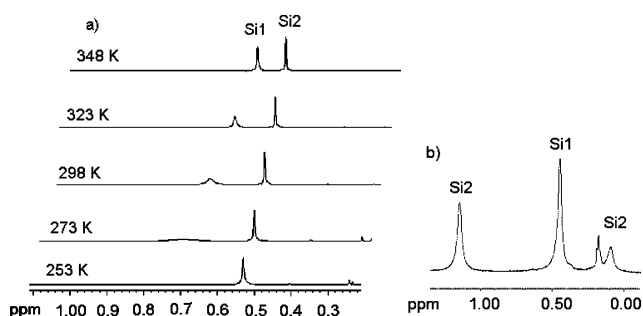


Figure 6. (a) Variable-temperature ^1H NMR spectra (C_7D_8) of **4**. Broadening of the SiMe_3 protons as the temperature is lowered. At 348 K two peaks are observed for the SiMe_3 protons labeled Si(1) and Si(2). When the sample is cooled, the protons for Si(1) broaden into the baseline. (b) ^1H NMR spectrum (C_7D_8) of **4** at the low-temperature limit (188 K). Below the coalescence temperature, two peaks are observed for the Si(1) protons at 1.13 and 0.09 ppm in a 5:1 ratio.

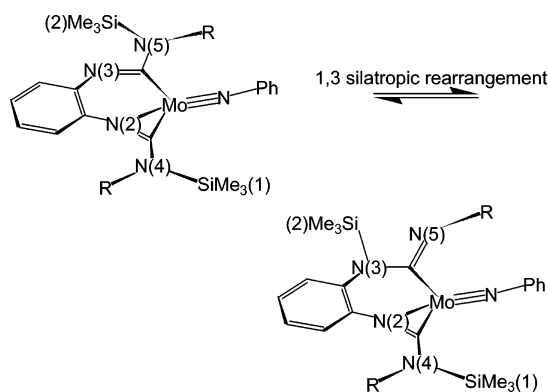
from the space-filling diagram, Si(2) interacts with both N(3) and N(5). These close contacts may explain the fluxionality of this molecule in solution (vide infra).

Dynamic Behavior of **4 in Solution.** Complex **4** is fluxional in solution. At room temperature two SiMe_3 protons can be observed at 0.52 (s, 9H) and 0.69 ppm (bs, 9H). When a C_7D_8 solution of **4** is heated to 348 K, the broad singlet sharpens and grows in intensity. The resonance observed at 0.69 ppm broadens into the baseline as this sample is cooled (Figure 6). Below the coalescence temperature (218 K) two peaks reemerge at 1.13 and 0.09 ppm in a 5:1 ratio. This fluxionality can be explained by a 1,3-silotropic rearrangement of the SiMe_3 group that has close contacts to two nitrogen atoms (Scheme 6).

Recall from Figure 6 that the group Si(2) has close contacts between both N(5) and N(3). Below the coalescence temperature the equilibrium shown in Scheme 6 will be frozen in solution and two species will be detected that differ in the position of $\text{SiMe}_3(2)$. In one

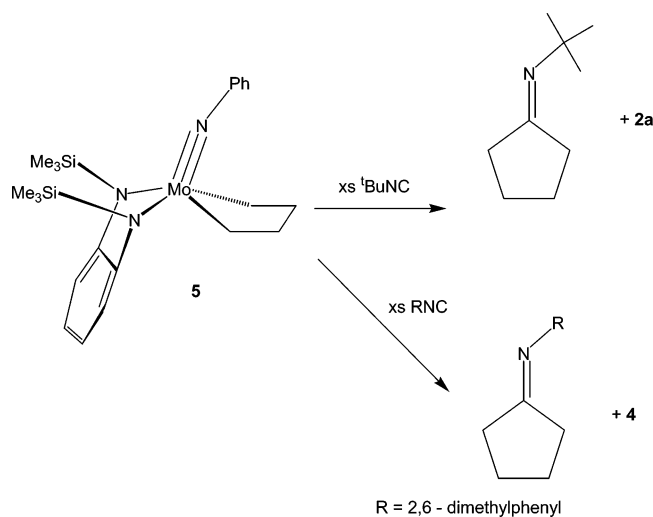
(37) Sanchez-Nieves, J.; Royo, P. *J. Organomet. Chem.* **2001**, *621*(1–2), 299–303.

(38) Gomez, M.; Gomezsal, P.; Jimenez, G.; Martin, A.; Royo, P.; Sancheznieves, J. *Organometallics* **1996**, *15*(16), 3579–3587.

Scheme 6^a

^a Coaxial ligands have been removed for clarity.

Scheme 7



position the group $\text{SiMe}_3(2)$ is bound to $\text{N}(5)$, and in the other position it is bound to $\text{N}(3)$. The populations of these sites are not equal; thus, the ratio of the two site populations is $\text{N}(5):\text{N}(3) = 5:1$. Above the coalescence temperature the chemical shifts for the SiMe_3 group are observed as an average of the chemical shifts for the two sites; i.e., above T_c the SiMe_3 group “feels” both $\text{N}(5)$ and $\text{N}(3)$. The exchange of unequally populated peaks has been described in more detail by Sandstrom in ref 39.

[2 + 2 + 1] Cycloaddition Reactions of Metallacycles with Alkyl and Aryl Isocyanides RNC. Our previous work with W alkyls and $^t\text{BuNC}$ seemed to suggest that isocyanide insertion in the case of W proceeded selectively into W -alkyl bonds over the W -diamide bond.¹⁵ We were interested in investigating whether isocyanide insertion was also competitive in the case of Mo -alkyl complexes; therefore, we pursued the reactions of the Mo metallacyclopentane complex **5** with isocyanides. Addition of 4.0 equiv of $^t\text{BuNC}$ to **5** results in the formation of **2a** and the iminocyclopentane molecule $\text{C}_5\text{H}_8\text{N}^t\text{Bu}$ (Scheme 7), while the addition of 5.0 equiv of 2,6-dimethylphenyl isocyanide to **5** results in the formation of the iminocyclopentane molecule $\text{C}_5\text{H}_8\text{N}(\text{xylyl})$ and **4**. The reactions outlined in Scheme 7 present a rare example of metal-mediated intermolecular [2 + 2 + 1] cycloaddition reactions of alkenes

and alkynes with alkyl and aryl isocyanides. In comparison with those for the related carbonylative cyclization, reports of related isocyanide-inserted cyclization are quite rare. Tamao *et al.* published the pioneering work of the $\text{Ni}(0)$ -induced cyclizations of diynes in 1989.⁴⁰ Since then, isocyanide insertion into zirconacyclopentadiene has been demonstrated by Takahashi *et al.*⁴¹ The Buchwald group^{42,43} and the Shibata group⁴⁴ have demonstrated the only two examples of catalytic coupling of alkynes and alkenes with alkyl isocyanides. We are currently exploring the catalytic possibilities of our complexes in the [2 + 2 + 1] cyclization of alkynes, alkenes, dienes, and diynes with alkyl and aryl isocyanides.

Summary and Conclusions

In this paper, we have synthesized rare examples of bis- and tris(isocyanide) complexes incorporating the isocyanide and imido moieties. We have also demonstrated that the chelating diamide ligand can be activated toward isocyanide insertion. This work is an extension of our ongoing studies on the importance of π ligand interactions and their role in influencing the outcome of chemical reactivity of group 6 complexes.

The insertion reactions seen between 2,6-dimethylphenyl isocyanide and the diamide ligand results from the π conflict that arises between the diamide nitrogen lone pairs and an occupied d orbital that results in the weakening of the $\text{Mo}-\text{N}(\text{diamide})$ bond and ultimately a lowering of the barrier to insertion. These results are promising, because they suggest that these insertion reactions may lead to the development of a catalyst for the carbonylation of amines.⁸ These species have been shown to be useful as precursors in organic synthesis. We are currently investigating the potential catalytic abilities of our complexes.

Experimental Section

All operations were conducted in an inert atmosphere using standard Schlenk techniques or in a nitrogen-filled drybox. Diethyl ether, pentane, toluene, and tetrahydrofuran were distilled under nitrogen from sodium or sodium benzophenone ketyl, stored over molecular sieves, and degassed prior to use. Ethylene was predried by passing the gas through a column of molecular sieves. Complexes **1**, **2a,b**, and **5** were synthesized according to published procedures.^{9–13} NMR spectra were recorded on Varian (300 MHz) Gemini300, VXR300, and Mercury300 instruments. Chemical shifts are reported in ppm relative to the ^1H and ^{13}C residues of the deuterated solvents. Elemental analyses were performed by Complete Analysis Laboratories Inc., Parsippany, NJ.

Synthesis of Bis(isocyanide) Complexes. [(*cis*- $^t\text{BuNC}$)- $\text{Mo}(\text{NPh})(o\text{-(Me}_3\text{SiN)}_2\text{C}_6\text{H}_4)]$ (2a**).** A pentane solution of **1** (1.00 g, 2.03 mmol) was charged with *tert*-butyl isocyanide (0.24 mL, 4.06 mmol). Green crystals of **2a** quickly precipitated. The suspension was filtered and washed several times with pentane. Excess solvent was removed in vacuo to afford

(40) Tamao, K.; Kobayashi, K.; Ito, Y. *J. Org. Chem.* **1989**, *54*, 3517.

(41) Takahashi, T.; Tsai, F. Y.; Li, Y. Z.; Nakajima, K. *Organometallics* **2001**, *20*, 4122.

(42) Berk, S. G.; Grossman, R. B.; Buchwald, S. L. *J. Am. Chem. Soc.* **1994**, *116*, 8593.

(43) Berk, S. G.; Grossman, R. B.; Buchwald, S. L. *J. Am. Chem. Soc.* **1993**, *115*, 4912.

(44) Shibata, T.; Yamashita, K.; Katayama, E.; Takagi, A. *Tetrahedron* **2002**, *58*, 8661.

(39) Sandstrom, J. *Dynamic NMR Spectroscopy*; Academic Press: London, 1982.

2a as a green microcrystalline material in 52% yield. Complex **2a** is thermally unstable in solution and in the solid state and disproportionates to **2a** and an unidentified material at 20 °C overnight. Because of this, elemental analysis was not attempted on this compound. Complex **2a** can be stored as a solid at -30 °C. ¹H NMR (C₆D₆): δ 0.73 (s, 18H, SiMe₃), 1.06 (s, 18H, ^tBuNC), 6.81 (tt, 2H, phenyl imido meta proton, 7.4, 1.2 Hz), 6.93 (t, 1H, phenyl imido para proton, 7.4 Hz), 7.05 (dd, 2H, *o*-phenylene diamide proton, 5.8, 3.3 Hz), 7.32 (dd, 2H, phenyl imido ortho proton, 7.5, 1.3 Hz), 7.48 (dd, 2H, *o*-phenylene diamide proton, 5.6, 3.4 Hz). ¹³C NMR (C₇D₈): 234.9, 187.1, 151.7, 128.6, 124.3, 123.7, 117.2, 117.1, 58.7, 30.3, 5.5.

[(*cis*-2,6-dimethylphenyl-NC)₂Mo(NPh)(*o*-(Me₃SiN)₂-C₆H₄)] (**2b**). A pentane solution of **1** (1.00 g, 2.03 mmol) was charged with 2,6-dimethylphenyl isocyanide (0.37 g, 2.82 mmol). Dark red crystals of **2b** quickly precipitated. The suspension was filtered and washed several times with pentane. Excess solvent was removed in vacuo to afford **2b** as a dark red microcrystalline material in 72% yield. ¹H NMR (C₆D₆): δ 7.52 (dd, 2H, *o*-phenylene diamide proton, 5.7, 3.5 Hz), 7.46 (d, 2H, phenyl imido ortho proton, 7.4 Hz), 7.07 (dd, 2H, *o*-phenylene diamide proton, 5.8, 3.4 Hz), 6.99 (t, 2H, phenyl imido meta proton, 7.2 Hz), 6.89 (t, 1H phenyl imido para proton, 7.3 Hz), 6.64 (ov multiplet, 6H, isocyanide phenyl protons), 2.12 (s, 12H, CH₃), 0.74 (s, 18H, SiMe₃). ¹³C NMR (C₇D₈): δ 200.9, 151.4, 131.5, 128.8, 125.2, 124.3, 117.8, 117.5, 18.8, 5.5. Complex **2b** loses a molecule of 2,6-dimethylphenyl isocyanide during the elemental analysis. Anal. Calcd for C₂₇H₃₆MoN₄Si₂: C, 57.02; H, 6.38; N, 9.85. Found: C, 57.20; H, 6.00; N, 9.80.

Synthesis of a Tris(isocyanide) Complex. (^tBuNC)₃Mo(NPh)(*o*-(Me₃SiN)₂-C₆H₄) (**3**). A diethyl ether solution of **1** (1.0 g, 2.03 mmol), was charged with 4 equiv of *tert*-butyl isocyanide (0.48 mL, 8.12 mmol) at room temperature. The reaction mixture quickly turned from green to purple and was stirred for 1 h. Small crystals of **3** started forming in solution during this time. Subsequently, the volume of the reaction was reduced and cooled for 1 h (-78 °C). Purple microcrystals of **3** were obtained by filtration at -78 °C. The solids were then dried overnight in vacuo, and **3** was obtained in 82% yield. MS: calcd for C₃₂H₅₂N₆Si₂Mo ([M - CH₃]⁺, *m/e* 674.285; found (FAB), *m/e* 674.280. ¹H NMR (C₆D₆): δ 0.58 (s, 9H, NSiMe₃), 0.77 (s, 9H, NSiMe₃), 0.93 (s, 18H, CN(C(CH₃)₃)), 1.17 (s, 9H, CN(C(CH₃)₃)), 6.81 (t, 1H, imido para hydrogen), 6.92 (m, 2H, (TMS)₂pda), 7.05 (t, 2H, imido meta hydrogen), 7.31 (d, 2H, imido ortho hydrogen), 7.42 (m, 2H, (TMS)₂pda). ¹³C NMR (C₇D₈, -10 °C): δ 4.02, 4.84, 30.02, 30.82, 56.26, 58.35, 112.63, 116.39, 116.53, 118.12, 120.52, 121.16, 122.60, 122.96, 150.86, 155.98, 157.72, 160.28.

Synthesis of a Chelating Imino Carbamoyl Complex (**4**). A pentane solution of **5** (1.00 g, 2.03 mmol) was treated with 2,6-dimethylphenyl isocyanide (1.16 g, 8.92 mmol); the solution was stirred overnight, and a yellowish brown powder precipitated. Washing this powder several times with cold pentane followed by recrystallization of the solids from pentane afforded **4** as red crystals in 46% yield. ¹H NMR (C₆D₆): δ 8.04 (dd, 2H, phenyl imido ortho proton, 8.2, 1.6 Hz), 7.23 (t, 2H, 2,6-dimethylphenyl isocyanide para proton, 8.4, 1.3 Hz), 7.2–6.5 (overlapping aromatic peaks, 16H), 5.43 (dd, 1H, phenyl imido para proton, 8.2, 1.6 Hz) 2.50 (s, 6H, CH₃ iminocarbamoyl), 1.94 (s, 12H, CH₃ 2,6-dimethylphenyl isocyanide), 1.87 (s, 6H, (CH₃ imino carbamoyl), 0.66 (bs, 9H, SiMe₃), 0.45 (s, 9H, SiMe₃). ¹³C NMR (C₇D₈): 203.3, 176.6, 157.7, 146.6, 146.2, 145.3, 137.9, 137.4, 136.4, 133.4, 129.1, 128.8, 127.3, 126.6, 125.3, 125.1, 125.0, 124.7, 124.0, 121.0, 120.8, 119.3, 119.1, 115.3, 20.0, 18.8, 18.2, 5.5, 0.78. Anal. Calcd for C₅₄H₆₄MoN₇-Si₂: C, 67.33; H, 6.70; N, 10.18. Found: C, 67.72; H, 6.95, N, 10.07.

X-ray Studies. Data were collected at 173 K on a Siemens SMART PLATFORM instrument equipped with a CCD area

Table 2. Crystal Data and Data Collection Parameters for (RNC)₂Mo(NPh)(*o*-(Me₃SiN)₂-C₆H₄) (2b**; R = 2,6-Dimethylphenyl), (^tBuNC)₃Mo(NPh)(*o*-(Me₃SiN)₂-C₆H₄) (**3**), and **4****

	2b	3	4
formula	C _{39.50} H ₄₉ Mo-N ₅ Si ₂	C ₃₃ H ₅₄ Mo-N ₆ Si ₂	C ₅₆ H ₇₃ Mo-N ₇ OSi ₂
formula wt	745.96	686.94	1036.35
cryst syst	triclinic	orthorhombic	triclinic
space group	<i>P</i> 1	<i>P</i> 2 ₁ 2 ₁ 2 ₁	<i>P</i> 1
<i>a</i> , Å	11.5484(9)	10.4614(6)	11.4653(12)
<i>b</i> , Å	11.8609(9)	18.571(1)	13.7990(14)
<i>c</i> , Å	14.8731(12)	19.715(1)	20.264(2)
<i>α</i> , deg	102.802(2)	90	90.006(2)
<i>β</i> , deg	93.928(2)	90	100.229(2)
<i>γ</i> , deg	94.868(2)	90	112.571(2)
<i>V</i> , Å ³	1971.4(3)	3830.1(4)	2905.1(5)
<i>Z</i>	2	4	2
<i>ρ</i> _{calcd} , Mg m ⁻³	1.257	1.191	1.185
temp, K		173(2)	
radiation		Mo Kα (0.710 73 Å)	
(wavelength)			
<i>R</i>	0.0349	0.0483	0.0484
<i>R</i> _w	0.0758	0.1086	0.0868

detector and a graphite monochromator utilizing Mo Kα radiation (λ = 0.710 73 Å). Cell parameters were refined using up to 8192 reflections. A full sphere of data (1850 frames) was collected using the ω-scan method (0.3° frame width). The first 50 frames were remeasured at the end of data collection to monitor instrument and crystal stability (the maximum correction on *I* was <1%). Absorption corrections by integration were applied on the basis of measured indexed crystal faces. Crystal data and data collection parameters for **2b**, **3**, and **4** are given in Table 2.

[(*cis*-2,6-dimethylphenyl-NC)₂Mo(NPh)(*o*-(Me₃SiN)₂-C₆H₄)] (**2b**). The structure was solved by direct methods in SHELXTL⁶⁴⁵ and refined using full-matrix least squares. The non-H atoms were treated anisotropically, whereas the hydrogen atoms were calculated in ideal positions riding on their respective carbon atoms. The asymmetric unit consists of the Mo complex and two half-molecules of ether (all ether molecules are located on inversion centers). The latter were disordered and could not be modeled properly; thus, the program SQUEEZE, a part of the PLATON package of crystallographic software, was used to calculate the solvent disorder area and remove its contribution to the overall intensity data. One of the Si atoms is disordered in two positions, Si(2) and Si(3). Accordingly, their methyl groups and the dimethylphenyl moiety are also disordered and were refined in two parts, with their site occupation factors dependently refined. A total of 621 parameters (with 36 restraints) was refined in the final cycle of refinement, using 6995 reflections with *I* > 2σ(*I*) to yield *R*₁ and *wR*₂ values of 4.84% and 9.81%, respectively. Refinement was done using *F*².

(^tBuNC)₃Mo(NPh)(*o*-(Me₃SiN)₂-C₆H₄) (**3**). The structure was solved by direct methods in SHELXT5 and refined using full-matrix least squares. The non-H atoms were treated anisotropically, whereas the hydrogen atoms were calculated in ideal positions riding on their respective carbon atoms. The SiMe₃ on N₂ is disordered and was refined in two parts with their occupation factors dependently refined. Also, the three methyl groups on C30 were disordered and were treated similarly. A total of 431 parameters (and 61 restraints) were refined in the final cycle of refinement using 5197 reflections with *I* > 2σ(*I*) to yield *R*₁ and *wR*₂ values of 4.83% and 8.54%, respectively. Refinement was done using *F*².

Iminocarbamoyl Complex (**4**). The structure was solved by direct methods in SHELXTL6 and refined using full-matrix least squares. The non-H atoms were treated anisotropically,

(45) Sheldrick, G. M. SHELXTL; Madison, WI, 1986.

whereas the hydrogen atoms were calculated in ideal positions riding on their respective carbon atoms. The asymmetric unit consists of the Mo complex and two half-molecules of ether (all ether molecules are located on inversion centers). The latter were disordered and could not be modeled properly; thus the program SQUEEZE, a part of the PLATON package of crystallographic software, was used to calculate the solvent disorder area and remove its contribution to the overall intensity data. One of the Si atoms is disordered in two positions, Si2 and Si3. Accordingly, their methyl groups and the dimethylphenyl moiety are also disordered and were refined in two parts, with their site occupation factors dependently refined. A total of 621 parameters (with 36 restraints) were refined in the final cycle of refinement using 6995 reflections with $I > 2\sigma(I)$ to yield R1 and wR2 values of 4.84% and 9.81%, respectively. Refinement was done using F^2 .

Computational Studies. Density functional theory (DFT) calculations were performed using the Gaussian 98W program package. Compound **3** was optimized using Morokuma's ONIOM method.^{34–36} For these ONIOM calculations a two-layer approach was used. For the inner layer, the *o*-phenylene group (*o*-C₆H₄) that links the two N atoms of the diamido ligand was simplified to a –CH=CH– carbon chain. The organic groups on the nitrogen atoms (SiMe₃ of the amido and phenyl group of the imido) were replaced by hydrogen atoms for simplicity. Becke's hybrid three-parameter functional

(B3LYP)⁴⁶ and the Los Alamos effective core potential (ECP) plus a standard double- ζ basis set (LANL2DZ)^{47,48} were used to describe the molybdenum center, and the Dunning/Huzinaga full double- ζ basis set (D95) was employed to describe all other atoms. Calculations were performed with default pruned fine grids for gradients and Hessians and default SCF convergence for geometry optimizations (10^{-8}).

Acknowledgment. We wish to acknowledge the National Science Foundation (Grant No. CHE-0094404) for the support of this work. K.A.A. wishes to acknowledge the National Science Foundation and the University of Florida for funding of the purchase of the X-ray equipment.

Supporting Information Available: Full details of experimental procedures and crystallographic data for compounds **2b**, **3**, and **4**, including tables of crystal data and data collection parameters, atomic coordinates, anisotropic displacement parameters, and all bond lengths and bond angles; CIF files for these compounds are also provided. This material is available free of charge via the Internet at <http://pubs.acs.org>.

OM0502436

(46) Becke, A. D. *J. Chem. Phys.* **1993**, *98*(2), 1372–1377.

(47) Hay, P. J.; Wadt, W. R. *J. Chem. Phys.* **1985**, *82*(1), 270–283.

(48) Hay, P. J.; Wadt, W. R. *J. Chem. Phys.* **1985**, *82*(1), 299–310.